Journal of ELECTRONIC MATERIALS, Vol. 46, No. 10, 2017
DOI: 10.1007/s11664-017-5613-7

On the Frequency and Voltage-Dependent Profiles of the Surface States and Series Resistance of Au/ZnO/n-Si Structures in a Wide Range of Frequency and Voltage

AFSOUN NIKRAVAN,[1,5] YOSEF BADALI,[2] ŞEMSETTIN ALTINDAL,[3] İBRAHIM USLU,[2] and İKRAM ORAK[4]

1.—Department of Environmental Engineering, Institute of Science, Hacettepe University, 06800 Ankara, Turkey. 2.—Department of Advanced Technologies, Institute of Science and Technology, Gazi University, Ankara, Turkey. 3.—Department of Physics, Faculty of Science, Gazi University, Ankara, Turkey. 4.—Department of Physics, Faculty of Science, Bingöl University, 12000 Bingöl, Turkey. 5.—e-mail: afsun.nikravan@gmail.com

In order to interpret the electrical characteristics of fabricated Au/ZnO/n-Si structures as a function of frequency and voltage well, their capacitance–voltage (C–V) and conductance–voltage (G/ω–V) measurements were carried out in a wide range of frequencies (0.7 kHz–2 MHz) and voltages (± 6 V) by 50 mV steps at room temperature. Both the C–V and G/ω–V plots have reverse, depletion, and accumulation regions such as a metal–insulator/oxide semiconductor (MIS or MOS) structures. The values of doped-donor atoms (N_D), Fermi energy level (E_F), barrier height (Φ_B), and series resistance (R_s) of the structure were obtained as a function of frequency and voltage. While the value of N_D decreases with increasing frequency almost as exponentially, the value of depletion width (W_D) increases. The values of C and G/ω increase with decreasing frequency because the surface states (N_{ss}) are able to follow the alternating current (AC) signal, resulting in excess capacitance (C_{ex}) and conductance (G_{ex}/ω), which depends on their relaxation time and the frequency of the AC signal. The voltage-dependent profiles of N_{ss} were obtained from both the high–low frequency capacitance and Hill-Colleman methods. The other important parameter R_s of the structure was also obtained from the Nicollian and Brews methods as a function of voltage.

Key words: Electrical properties, interfacial layer, voltage-dependent of surface states and series resistance

INTRODUCTION

In recent years, metal–semiconductor (MS) structures with interfacial layers such as polyvinyl alcohol (PVA), $Bi_4Ti_3O_{12}$ (BTO), perylenetetracarboxylic dianhydride (PTCDA), CdS-PVA, zinc-oxide (ZnO), and graphene-doped PVA structures, which are called metal-polymer-semiconductors (MPS), metal-ferroelectric-semiconductors (MFS), MIS structures, have been used instead of conventional MS-type structures in electronic and optoelectronic devices.[1–7] MIS is the most convenient structure and demonstrates compatibility between the insulator and semiconductor layers.[8] The quality and performance of these structures are dependent on various parameters. Among them are the interface quality, doping concentration level, frequency, bias voltage or electric field, series resistance (R_s), surface states (N_{ss}), and the homogeneity of barrier height (BH) between metal and semiconductor are more effective on the electric and dielectric properties of these devices. As reported in many studies, the conduction mechanism and formation of BH at M/S interface could be changed by the use of an

(Received September 19, 2016; accepted May 22, 2017; published online June 5, 2017)

appropriate interlayer between semiconductor and metal.[9] There are numerous methods to determine the density distribution of N_{ss} and R_s.[10–16] Among them the best, simplest, and the most accurate methods is low–high frequency capacitance (CLF–CHF) and Nicollian and Brews techniques, respectively.[17] Investigation of N_{ss} and R_s as a function of frequency and voltage in these devices is one of the most popular topics in the literature.[10,14,18,19] The interfacial layers and interface states, N_{ss}, are effective especially at lower and intermediate frequencies in the inversion and depletion regions; on the other hand, R_s is only effective at higher frequencies in strong accumulation regions. When voltage is applied on the diode, it will be shared between interfacial layer and series resistance (R_s) and depletion layer.[8,20] At low frequencies, the charge carriers at surface states and their relaxation times (τ) are lower than the period (T). Thus, these charges can easily follow the external alternating signal, yielding an excess capacitance and conductance in addition to the measured capacitance and conductance, especially in inversion and depletion regions.

One of the most significant and extensively used materials in electronic applications is ZnO due to its chemical and physical properties, radiation resistance, non-toxicity, natural abundance, 60 meV excitation binding energy, and a large direct band gap around 3.4 (eV). It is well known that ZnO acts as an n-type semiconductor owing to deficiency of oxygen. The binding energy of ZnO is almost three times larger than that of gallium nitrate (GaN), and its biexciton formation energy is almost 15 meV, which is also much larger than GaN. Usually, oxygen vacancies or zinc interstitials are responsible for low resistivity to pure zinc oxide. Because of these important properties, it has many application areas in technology such as Schottky-type diodes (SDs), solar cells (SCs), chemical sensors (CSs), light-emitting diodes (LEDs), UV photodetectors, and laser diodes.[21–26] A variety of methods for chemical synthesis have been used by several researchers to synthesize nano/micro-crystals such as solvothermal, hydrothermal, self-assembly, chemical vapor deposition (CVD), pulsed laser deposition (PLD), radio frequency sputtering (RFS), and sol–gel.[10,23,24]

In the present study, MIS-type structures consisting of an Au/ZnO/n-Si have been investigated as a function of the frequency and applied bias voltage. The capacitance–voltage (C–V) and conductance–voltage (G/ω–V) measurements were carried out in the frequency range of 0.7 kHz and 2 MHz and between −6 V and 6 V applied bias voltages by 50 mV steps at room temperature. The important electrical parameters such as concentration of donor atoms (N_D), Fermi energy level (E_F), barrier height (Φ_B), and W_D values of the structure were obtained from the slope and by the extrapolation of the linear region of the C^{-2} versus V plots for each frequency. The voltage dependent profiles of N_{ss} and R_s of the structure were calculated from the high–low frequency capacitance and Nicollian and Brews methods, respectively.

EXPERIMENTAL PROCEDURES

Au/ZnO/n-Si structures have been fabricated on a phosphorus-doped (n-type) Si wafer with (100) surface orientation, 300 μm thickness, 2 inch (= 5.08 cm) diameter, and 0.1 Ω cm resistivity. For the fabrication processes, the n-Si wafer was ultrasonically cleaned in boiling trichloroethylene, acetone, and ethanol consecutively and then etched in a sequence of H_2SO_4 and H_2O_2, 20% HF, a solution of $6HNO_3$:1HF:$35H_2O_2$, 20% HF, and finally quenched in de-ionized (DI) water at 18 MΩ cm for 5 min. The backside of the wafer was immediately deposited by thermally evaporated high purity gold (99.999%) with a thickness of ∼1500 Å under a pressure of $\sim 2 \times 10^{-6}$ Torr in a high vacuum metal-evaporation system. To get a low resistivity back ohmic contact, n-Si/Au structure was annealed at the 500°C for 30 min in flowing dry nitrogen in order for preventing any oxidation of n-Si surface. After the formation of the ohmic contact, the interfacial ZnO layer was grown on the front of the n-Si surface by RF Sputtering. A ZnO sputtering target (diam. × thickness 3.00 in. × 0.125 in., 99.99% trace metals basis) was used for the experiment because of its poor thermal conductivity. When the pressure of the system is about 5×10^{-6} Torr, pure argon gas (99.99%) is sent to the vacuum chamber at constant speed (∼80–100 ccm). Then it remains until the pressure reaches 30 mTorr. These conditions are helf for 5 min to balance the system. Then a power of about 150 W was applied and at stable frequency 13.6 MHz when shutter is closed. Finally, the shutter is opened and the rectifier contacts are formed by thermal evaporation with 1500 Å thickness.

After the rectifier contacts are formed, high purity Au (∼2 mm diameter) is decorated onto the ZnO. Thus, the fabrication processes of Au/ZnO/n-Si structures are completed. The thickness of the ohmic and rectifier metal contacts and the deposition rates were monitored with the help of a quartz crystal thickness monitor. In order to perform electrical measurements, Au/ZnO/n-Si structures were mounted on a copper (Cu) holder with the help of silver (Ag) paste and were made with the upper electrodes by the use of tiny Ag-coated Cu-wires with silver paste. The interfacial layer thickness (di) was determined as 30 nm using a UCF Stylus profilometer. The C–V–f and G/ω–V–f measurements of the structure were measured using a computerized HP 4192A LF impedance analyzer in the wide range of frequency and voltage. The measurements were done with the help of a microcomputer through an IEEE-488 AC/DC converter card in a JANES VPF-475 Cryostat at 10^{-3} Torr.

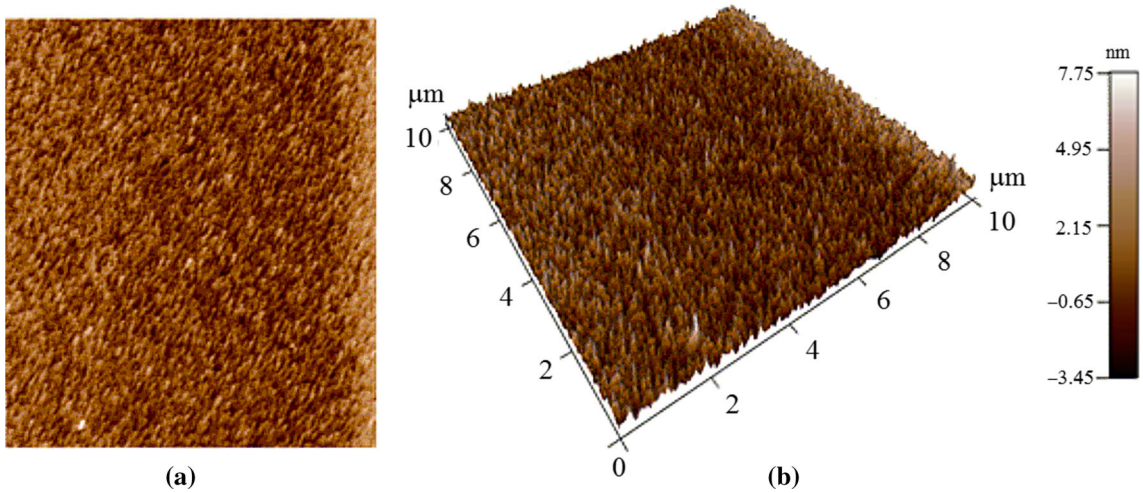

Fig. 1. (a, b) 2D and 3D the surface morphology of deposited 10 nm ZnO on the substrate, the RMS value is 1.29 nm.

RESULTS AND DISCUSSION

ZnO Thin Film Characterization

Both the 2D and 3D atomic force microscopy (AFM) images of the ZnO thin film surface on the n-Si scanned in 10 μm × 10 μm areas can be seen in Fig. 1a and b for surface morphology of the structure. There is good homogeneity and a uniform distribution which consists of spheroid shaped nano-crystallize on the surface of the device without any holes and cracks. Root mean square (RMS) roughness value of the device is about 1.29 nm. This value is very suitable for an electronic device. It is well known that the use of deposition/growth method of ZnO thin films on silicon or other semiconductors is more important.

The Calculation of Main Electrical Parameters for Various Frequencies

It is a well-known fact that the C–V and G/ω–V measurements of MIS and MOS structures at a single frequency or a very narrow frequency or voltage range cannot give us detailed information on the conduction mechanisms, the formation of BH and the N_{ss} between metal and semiconductor. For this reason, both C–V and G/ω–V measurements were carried out in the frequency range of 0.7 kHz–2 MHz whereas the applied voltage swept from −6 V to 6 V by 100 mV steps. Figures 2a, b, and 3 show the C–V and G/ω–V characteristics of the Au/ZnO/n-Si structure, respectively. As can be seen from these figures, the plots of both the C–V and G/ω–V depict the inversion, depletion and accumulation regions as in an MIS or MOS structure behavior. From the shape of the curves in the plots, it is clear that both the value of C and G/ω decrease with increasing frequency.

The change in capacitance becomes more pronounced in the depletion region at low frequencies due especially to the existence of a particular distribution of N_{ss} at the ZnO/n-Si interface, surface, or dipole polarizations and hopping mechanisms.[22,23] At low and intermediate frequencies, the obtained higher values of C and G/ω can be ascribed to an increase in the polarization and the follow rate of surface states to ac signal. It is well known that at low frequencies, the charges at surface states or traps can easily follow the external ac signal and so yield an excess capacitance ($C_{ex.}$) and conductance ($G_{ex.}/\omega$).[17,27–30] The features of these plots can also be attributed the relaxation polarization and surface states and their lifetime.[28–31] At high frequencies, these states cannot follow the ac signal and so in this case their contribution to the total capacitance is negligibly small.

Since localized electronic states exist at the interface, electronic device behavior such as C–V and G/ω–V characteristics deviated from the ideal case. As seen in Fig. 2a, at low frequencies, the C–V plots have two distinctive peaks, corresponding to the depletion and accumulation region; however, the peak in the forward bias C–V plots disappears at high frequencies ($f \geq 30$ kHz). This two-peak behavior can be ascribed to the particular density distribution of surface states at ZnO/n-Si interface. The magnitude of peak in the depletion region is gradually decreased with increasing frequency and shifts towards the positive bias region due to deep level states and series resistance.[17] According to this work, such peak behavior, which is called an anomalous peak in the literature, is the result of the existence of surface states and series resistance of the structure. The origin of such a peak variation in the C–V plots has been ascribed to the surface states by Ho et al.,[32] but Werner et al.[33] have shown that the observed peak in the forward bias C–V plot is due to R_s. On the other hand, Chattopadhyay et al.[34] have theoretically shown that the peak value of the capacitance changes both R_s and N_{ss}. These results were confirmed that the values of R_s

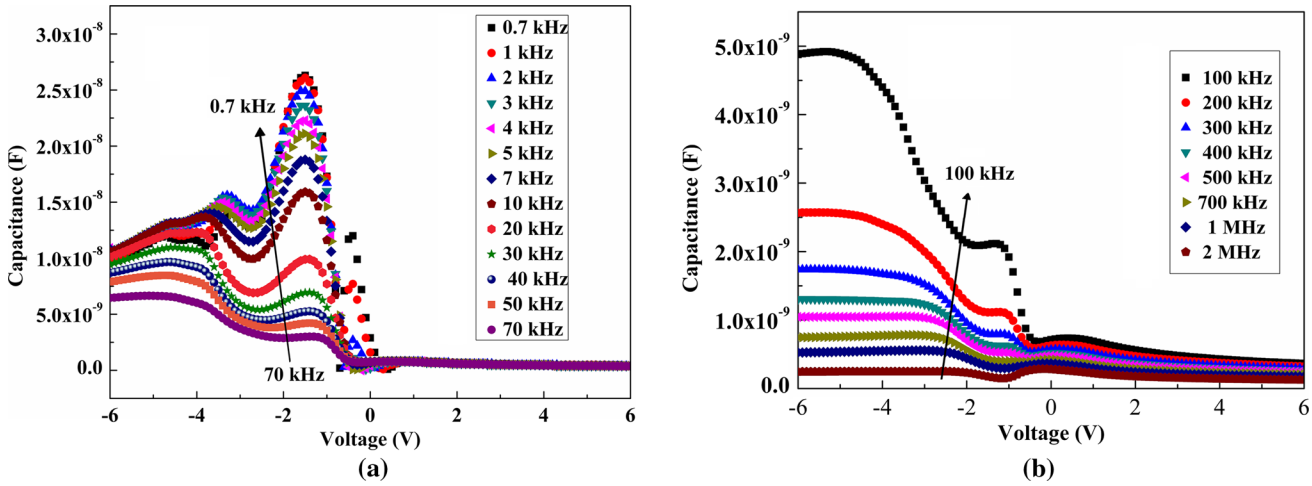

Fig. 2. Depicts the *C–V* characteristics of the Au/ZnO/n-Si structure at room temperature; (a) for low frequencies and (b) for high frequencies.

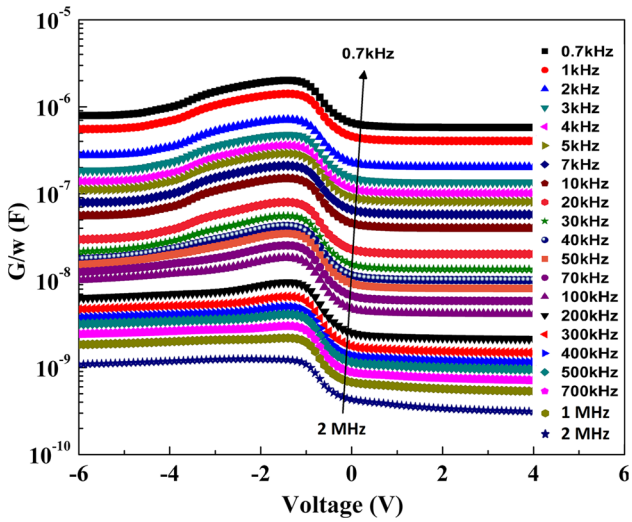

Fig. 3. Depicts the G/ω–V characteristics of the Au/ZnO/n-Si structure for various frequencies at room temperature.

and N_{ss} are two important parameters and influenced the electrical characteristics. Therefore, they should be taken into the calculations of electrical and dielectric properties of these structures to increase the accuracy and reliability of the results.

Because the resistance (R_i) of the diodes have important effect on the electrical characteristics, the R_i–V plot was obtained from the measured C and G data by using Nicollian–Brews method[17,27] for each frequency and was presented in Fig. 4. According to this method, the real value of series resistance of the MIS type structure was corresponding to the strong accumulation region. Accordingly, the real value of R_s can be calculated from the following equation:

$$R_s = \frac{G_{ma}}{G_{ma}^2 + \omega^2 C_{ma}^2} \qquad (1)$$

where $\omega = (2\pi f)$ is the angular frequency, C_{ma} and G_{ma} are the capacitance and conductance values at strong accumulation region of the structure. In addition, the voltage dependent profile of R_i can be obtained by using Eq. 1. As shown in Fig. 4, the R_i–V plots have almost a U shape behavior, especially at low frequencies due to the particular density distribution profile of surface states. The real value of R_s was obtained as 286.39 Ω at 0.7 kHz and 69.67 Ω at 2 MHz for −6 V and 120.19 Ω at 0.7 kHz and 61.80 Ω at 2 MHz for −2 V, respectively. It is obvious that the value of resistance is not only a strong function of frequency but also the voltage, and it decreases with increasing frequency for each bias voltage as seen from the inset in Fig. 4. The higher values of R_s at low frequencies are the result of the existence of surface states and surface or dipole polarization, but their effect is as low as it could be neglected at sufficiently high frequencies ($f \geq 1$ MHz). Therefore, the real value of R_s should be obtained at a high enough frequency in a strong accumulation region. These results confirmed that R_s is effective only in accumulation region, whereas N_{ss} are effective in both depletion and inversion regions.

In the MS, MIS, and MPS type structures or solar cells, the value of the depletion layer capacitance varies with the applied bias voltage (V) as expressed by the following relation[17]:

$$C^{-2} = \left(\frac{2}{q\varepsilon_s\varepsilon_o N_D A^2}\right) V_D - kT/q - V, \qquad (2)$$

where N_D is the concentration of doping donor atoms (P), V_D is the diffusion potential, A is the rectifier contact area in cm^{-2}, ε_s (= $11.8\varepsilon_o$) is the permittivity of semiconductor and ε_o is the permittivity of vacuum or free space. In order to determine some main electrical parameters of the structure, such as diffusion potential (V_D), N_D, Fermi energy level (E_F), maximum electric field (E_m), depletion

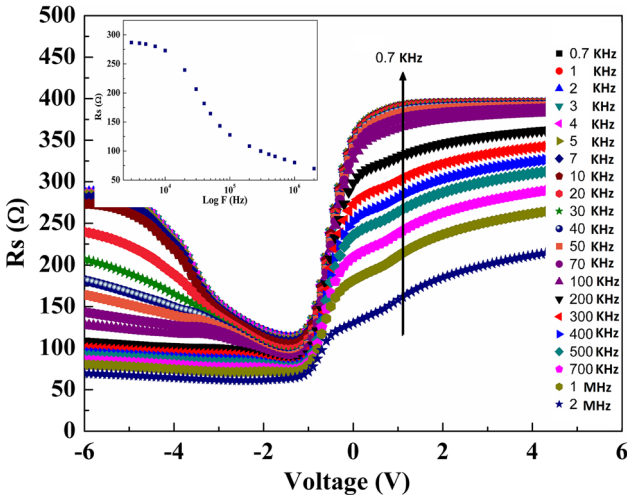

Fig. 4. The R_s–V plots of the Au/ZnO/n-Si structure for various frequencies at room temperature.

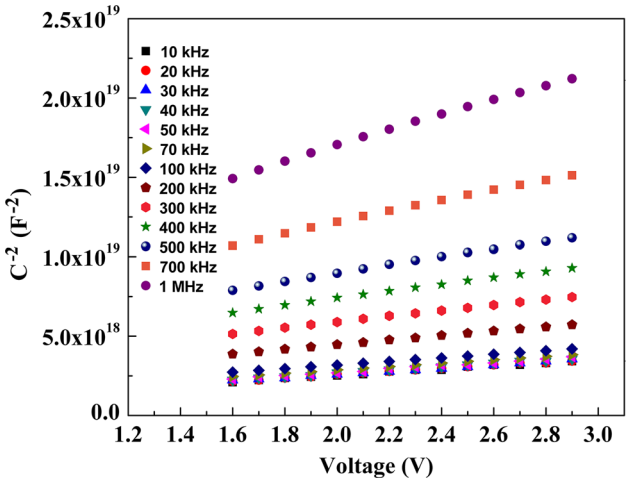

Fig. 5. The C^{-2} versus V plot of the Au/ZnO/n-Si structure for various frequencies at room temperature.

layer width (W_D), and barrier height (Φ_{C-V}), as a function of frequency, the C^{-2} versus V plot was drawn for all frequencies and presented for intermediate and high frequencies 10 kHz–1 MHz at room temperature (Fig. 5). As shown in Fig. 5, the C^{-2}–V plots of the Au/ZnO/n-Si structure has a good linear behavior in the wide range of applied bias voltage for each frequency.

The voltage or x-axis interception in the reverse bias of the C^{-2}–V plot gives directly the value of V_o and it is related to the diffusion potential ($V_D = V_o + kT/q$). We have estimated the values of V_o and N_D from the intercept and slope $\left(= 2/\left(q\varepsilon_s\varepsilon_o N_D A^2\right)\right)$ of the C^{-2}–V plots (Fig. 5). Subsequently, the value of E_F was also calculated for the structure by using the following equation for each frequency:

$$E_F = \frac{\kappa T}{q}\ln\left(\frac{N_C}{N_D}\right) \tag{3}$$

With,

$$N_C = 4.82 \times 10^{15} T^{3/2}(m_e^*/m_0)^{3/2} \tag{4}$$

In Eq. 4, N_C is the effective density of states in the Si conductance band (E_c), $m_e^* = 0.98\ m_o$ is the effective mass of the electron,[17] and $m_o = 9.1 \times 10^{-31}$ kg is the rest mass of the electron. Accordingly, the value of Φ_{C-V} was obtained by using the following relations.[12,15] The values of image force lowering of BH ($\Delta\Phi_B$) and the maximum electric field (E_m) were also obtained from the following relations, respectively:

$$\Delta\Phi_B = \left[\frac{qE_m}{4\pi\varepsilon_s\varepsilon_o}\right]^{\frac{1}{2}} \tag{5}$$

$$E_m = \left[\frac{2qN_D V_0}{\varepsilon_s\varepsilon_o}\right] \tag{6}$$

Thus, the frequency dependent value of Φ_{C-V} for the fabricated Au/ZnO/n-Si structure was obtained as a function of frequency using Eq. 7 and tabulated in Table I.

$$\Phi_{C-V} = \left(V_0 + \frac{kT}{q}\right) + E_F - \Delta\Phi_B = V_D + E_F - \Delta\Phi_B \tag{7}$$

The resulting experimental values of V_D, N_D, E_F, E_m, W_D and Φ_{C-V} of the Au/ZnO/n-Si structure for each frequency at room temperature were tabulated in Table I. As can be seen in Table I, all of these parameters are a strong function of frequency, but the value of image force lowering of BH ($\Delta\Phi_B$) is very low when it is compared with E_F and Φ_{C-V} due to the moderate doping density of donor atoms.

As can be seen in Fig. 5 and Table I, while the value of N_D decreases with increasing frequency almost exponentially, the value of W_D increases. Furthermore, the value of R_s obtained from Eq. 1 at a strong accumulation region (−6 V), decreases with increasing frequency, as expected. The obtained experimental high values of N_D and R_s at low and intermediate frequencies can be attributed to the existence of surface charges located at traps and the interfacial layer. The change in these parameters with frequency is especially resulting from N_{ss} and their relaxation time (τ).[3–8,17] If the period ($= 1/f$) is lower than the τ of traps or surface states, the charges in these states can follow the alternative signal and so we contributed to the measured total capacitance and conductance. Therefore, the contribution of C and G by surface states is very important especially at low frequencies. Contrarily, the value of R_s becomes very effective at high frequency, especially in accumulation region (Fig. 6).

Table I. Frequency dependent V_D, N_D, E_F, E_m, W_D , and Φ_{C-V} values of the Au/ZnO/n-Si structure obtained from the C^{-2} versus V plot at room temperature

Frequency (Hz)	V_o (V)	N_D (cm^{-3})	E_F (eV)	E_m (V/cm)	W_D (cm)	$\Delta\Phi_B$ (eV)	Φ_B (eV)	$R_s(-2\ V)\ \Omega$
1×10^4	0.536	1.22×10^{16}	0.194	4.47×10^4	2.40×10^{-5}	0.080	0.674	112.32
2×10^4	0.550	1.22×10^{16}	0.194	4.63×10^4	2.48×10^{-5}	0.082	0.688	106.11
3×10^4	0.560	1.19×10^{16}	0.194	4.48×10^4	2.46×10^{-5}	0.080	0.698	102.52
4×10^4	0.582	1.18×10^{16}	0.194	4.58×10^4	2.54×10^{-5}	0.081	0.720	100.15
5×10^4	0.609	1.17×10^{16}	0.195	4.67×10^4	2.61×10^{-5}	0.082	0.746	98.43
7×10^4	0.645	1.15×10^{16}	0.195	5.03×10^4	2.87×10^{-5}	0.085	0.782	96.01
1×10^5	0.700	1.07×10^{16}	0.197	5.19×10^4	3.15×10^{-5}	0.086	0.839	93.56
2×10^5	0.790	8.49×10^{15}	0.203	5.41×10^4	4.16×10^{-5}	0.088	0.937	88.68
3×10^5	0.840	6.82×10^{15}	0.208	5.22×10^4	4.99×10^{-5}	0.087	0.995	85.43
4×10^5	0.870	5.62×10^{15}	0.213	4.95×10^4	5.75×10^{-5}	0.084	1.033	82.76
5×10^5	0.920	4.76×10^{15}	0.217	4.71×10^4	6.45×10^{-5}	0.082	1.089	80.44
7×10^5	0.950	3.57×10^{15}	0.224	4.15×10^4	7.59×10^{-5}	0.077	1.131	76.5
1×10^6	0.978	2.51×10^{15}	0.233	3.42×10^4	8.88×10^{-5}	0.070	1.173	71.83

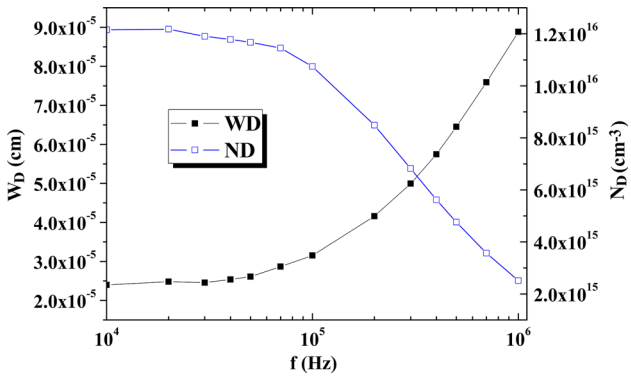

Fig. 6. The variation of N_D and W_D with frequency in the Au/ZnO/n-Si structure at room temperature.

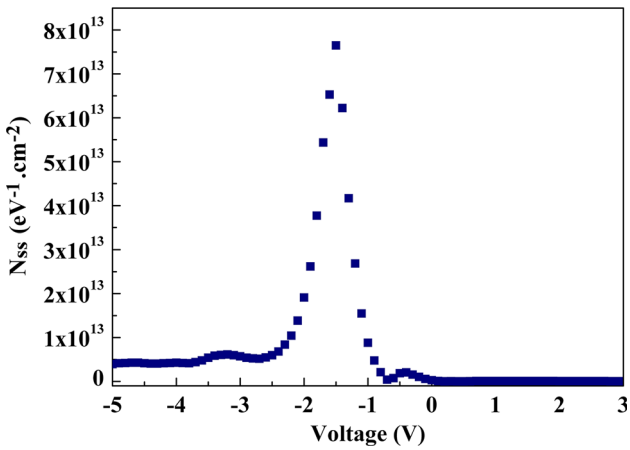

Fig. 7. The voltage dependent profile of Nss in the Au/ZnO/n-Si structure at room temperature.

The Obtaining Voltage and Frequency Dependent Profiles of Surface States

The voltage dependent profile of N_{ss} can be obtained from the adequately low and high frequency capacitance 1 kHz–1 MHz plots, and this method is known as low–high frequency capacitance (C_{LF}–C_{HF}) method.[17,27] This method is simple, not time consuming, and can supply enough accurate results approximate to the more accurate and complicated of the admittance method. Therefore, in this study, the voltage dependent profile of N_{ss} was the obtained (C_{LF}–C_{HF}) method and was given in Fig. 7. It permits the determination of N_{ss} from the use of only two C–V plots. In the equivalent circuit of MIS or MOS type structures, the interfacial layer capacitance C_i is connected in series with the parallel combination of the N_{ss} capacitance (C_{ss}) and the space charge capacitance (C_{sc}).[27] It is expected that the carrier charges at traps cannot respond to the external ac signal and do not contribute to the total capacitance directly, but at low frequencies they can easily follow the ac signal. Therefore, the voltage dependent profile of N_{ss} was obtained from the following relation:

$$N_{ss} = C_{ss}/qA = (1/qA)[1/C_{LF} - 1/C_i]^{-1} - [1/C_{HF} - 1/C_i]^{-1}, \quad (8)$$

where C_i is the interfacial layer capacitance and others are known quantities in the literature. In Fig. 7, it is shown that the N_{ss}–V plot has a distinctive peak at about (−1.5 V). The peak behavior of N_{ss}–V can be attributed to a certain density distribution of the surface states between interfacial ZnO and n-Si.[17,25–28] The resulting mean value of N_{ss} ($\approx 2\times10^{13}$ eV^{-1} cm^{-2}) is more suitable for an electronic device. According to us, these low values of N_{ss} are the result of the passivation effect of the used ZnO interfacial layer.

In order to see the frequency response of N_{ss}, frequency dependent profile of N_{ss} was obtained from the Hill-Coleman method.[35] According to this method, the density of N_{ss} can be approximated using a set of the C–V–f and G/ω–V–f

measurements when these plots have a peak in depletion or accumulation region. This method is simpler and quicker as compared to the admittance method developed by Nicollian and Goetzberger. An equation governing the N_{ss} at a single frequency was given as[35]:

$$N_{ss} = \frac{2}{qA}\left(\frac{(Gm/\omega)_{max}}{((Gm/\omega)_{max}/C_{ox})^2 + (1 - C_m/C_{ox})}\right) \quad (9)$$

The frequency dependent values of N_{ss} obtained from Eq. 9 were given in Table II and Fig. 8, respectively. As shown in Fig. 8, at low frequencies the value of N_{ss} is larger than the high frequencies as expected and semi-logarithmic N_{ss} versus *Log f* plot has a peak at about 10^5 Hz.

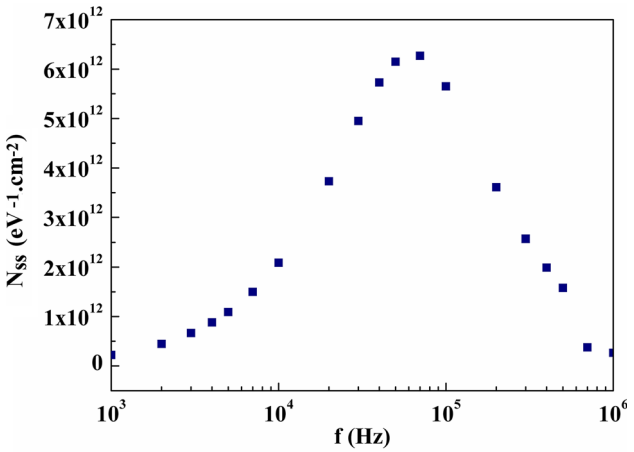

Fig. 8. The frequency dependent profile of the surface state density of the Au/ZnO/n-Si structure determined by the Hill-Coleman method at room temperature.

Figure 7 Voltage dependent profile of N_{ss} for the Au/ZnO/n-Si structure obtained from high-low frequency capacitance method at room temperature. The surface states can store charges and leads to an associated the excess capacitance (C_{ss}) and conductance (G_{ss}/ω). Namely, if the applied frequency is lower than or equal to the τ of the charge at surface state, then these charges at traps will contribute to the total measured capacitance and conductance, and as can be seen in Table II, this contribution decreases with increasing frequency.[36,37] At high enough frequency ($f \geq 1$ MHz), both the contribution of N_{ss} and polarization to the measured of C and G is considerably low. These surface states also cause a bias shift and frequency dispersion both in C–V and G/ω–V plots. Therefore, it is very important to consider the effect of the frequency and voltage to examine the frequency dispersion of admittance measurements in detail, which include capacitance and conductance in the MS, MIS, MPS, and MFS type structures.

As can be seen in Fig. 8 and Table II, the obtained values of N_{ss} from Hill-Coleman method were changed from 2.23×10^{11} $eV^{-1}cm^{-2}$ to 6.27×10^{12} $eV^{-1}cm^{-2}$. When these values are compared to the literature, they are considerably lower and very suitable for an electronic device.[38–41] For instance, Asghar et al.[39] obtained the values of N_{ss} for Au Schottky contact on ZnO grown by molecular beam epitaxy (MBE) and they changed almost from the 2.0×10^{12} $eV^{-1}cm^{-2}$ to 1.9×10^{13} $eV^{-1}cm^{-2}$.

Table II. Frequency dependent of N_{ss} the Au/ZnO/n-Si structure obtained from the Hill-Coleman method at room temperature

Frequency (Hz)	Vm (V)	Cm (F)	G/ω (F)	N_{ss} (eV-1.cm-2)	R_s (at Vm) (Ω)
700	−1.5	2.63×10^{-8}	2.01×10^{-6}	1.56×10^{11}	113.27
1000	−1.5	2.61×10^{-8}	1.41×10^{-6}	2.23×10^{11}	113.17
2000	−1.6	2.49×10^{-8}	7.02×10^{-7}	4.47×10^{11}	113.29
3000	−1.6	2.36×10^{-8}	4.71×10^{-7}	6.66×10^{11}	112.42
4000	−1.6	2.22×10^{-8}	3.56×10^{-7}	8.81×10^{11}	111.46
5000	−1.6	2.10×10^{-8}	2.87×10^{-7}	1.09×10^{12}	110.42
7000	−1.6	1.86×10^{-8}	2.08×10^{-7}	1.50×10^{12}	108.32
10,000	−1.6	1.57×10^{-8}	1.49×10^{-7}	2.09×10^{12}	105.44
20,000	−1.5	9.90×10^{-9}	7.99×10^{-8}	3.73×10^{12}	98.17
30,000	−1.4	6.95×10^{-9}	5.53×10^{-8}	4.95×10^{12}	94.42
40,000	−1.4	5.27×10^{-9}	4.26×10^{-8}	5.73×10^{12}	92.08
50,000	−1.4	4.22×10^{-9}	3.47×10^{-8}	6.15×10^{12}	90.44
70,000	−1.3	3.00×10^{-9}	2.52×10^{-8}	6.27×10^{12}	88.85
100,000	−1.2	2.10×10^{-9}	1.78×10^{-8}	5.65×10^{12}	88.36
200,000	−1.2	1.11×10^{-9}	9.33×10^{-9}	3.61×10^{12}	84.16
300,000	−1.2	7.92×10^{-10}	6.40×10^{-9}	2.57×10^{12}	81.64
400,000	−1.2	6.27×10^{-10}	4.91×10^{-9}	1.99×10^{12}	79.75
500,000	−1.1	5.24×10^{-10}	3.87×10^{-9}	1.58×10^{12}	80.82
700,000	−0.1	4.20×10^{-10}	9.16×10^{-10}	3.77×10^{11}	205.10
1,000,000	−0.3	3.61×10^{-10}	6.47×10^{-10}	2.66×10^{11}	168.43
2,000,000	−0.3	2.82×10^{-10}	4.06×10^{-10}	1.66×10^{11}	122.85

Moreover, the mean values of N_{ss} were found as 6.46×10^{14} $eV^{-1}cm^{-2}$ and 2.05×10^{15} $eV^{-1}cm^{-2}$ by using the forward bias current–voltage measurements of the ZnO based Schottky contacts grown by radio frequency (RF) sputtering method by taking into account voltage dependent ideality factor and effective barrier height at room temperature by Singh et al.[40] and Rajan,[41] respectively. The higher values of N_{ss} and R_s lead to degrading the performance of electronic devices.

CONCLUSION

To interpret the frequency and voltage dependence accurately on the main electrical parameters of the Au/ZnO/n-Si structure, the C–V and G/ω–V measurements were performed in a wide range of frequency (0.7 kHz–2 MHz) and voltage (±6 V) in 50 mV steps. Experimental results show that C–V and G/ω–V plots have reversed depletion and accumulation regions, and both the value of C and G/ω depend strongly on frequency and voltage, especially in depletion and accumulation regions. The higher values of capacitance and conductance at low frequencies were attributed to the existence of N_{ss} and their relaxation time, surface and dipole polarizations. In order to determine the effects of N_{ss} and R_s on the electrical characteristics, their voltage and frequency dependence profiles for the Au/ZnO/n-Si structure were obtained from the (high-low frequency capacitance and Hill–Coleman methods) and Nicollian and Brews method, respectively. The mean values of N_{ss} obtained from each method are in good agreement with each other. While the value of N_D decreases with increasing frequency almost exponentially, the values of W_D and R_s decrease with increasing frequency because in enough high frequency ($f \geq 1$ MHz), both the contribution of N_{ss} and polarization to the measured of C and G start to decrease. Experimental results confirm that the existence of N_{ss}, R_s and interfacial ZnO layer at M/S interface are more effective on the electrical characteristics. Therefore, the effects of these parameters should be taken into account in the calculation of electrical characteristics. Surface states and polarization also cause a bias shift and frequency dispersion both in C–V and G/ω–V plots. For these reasons, the studies on frequency, voltage, and polarization dependent admittance measurements which are included capacitance and conductance in the MS, MIS, MPS, and MFS type structures is vitally important to get reliable and accurate results associated with their electrical and dielectric properties.

ACKNOWLEDGEMENT

ARTEMIZ Research and Development (R&D) Company supported this work. ARTEMIZ is an establishment, which is financially supported by Small and Medium Enterprises Development Organization (KOSGEB), Republic of Turkey.

REFERENCES

1. G. Ersöz, I. Yücedag, Y. Azizian-Kalandaragh, I. Orak, and S. Altındal, *IEEE Trans. Electron Dev.* 63, 2948 (2016).
2. S. Demirezen, A. Kaya, Ö. Vural, and Ş. Altındal, *Mater. Sci. Semicond. Process.* 33, 140 (2015).
3. Y.Ş. Asar, T. Asar, Ş. Altındal, and S. Özçelik, *Phil. Mag.* 95, 2885 (2015).
4. S.A. Yerişkin, M. Balbasi, and A. Tataroglu, *J. Appl. Poly. Sci.* 133 (2016). doi:10.1002/app.43827.
5. M.M. Bulbul, S. Altindal, F. Parlakturk, and A. Tataroglu, *Surf. Interface. Anal.*, 43, 1561 (2011).
6. H. Tecimer, H. Uslu, Z.A. Alahmed, F. Yakuphanoğlu, and Ş. Altındal, *Compos. Part B: Eng.* 57, 25 (2014).
7. Y.S. Altindal, H.I. Unal, and S. Bekir, *J. Appl. Poly. Sci.* 120, 390 (2011).
8. İ. Taşçıoğlu, M. Soylu, Ş. Altındal, A.A. Al-Ghamdi, and F. Yakuphanoglu, *J. Alloys Compd.* 541, 462 (2012).
9. M.K. Hudait and S.B. Krupanidhi, *Solid-State Electron* 44, 1089 (2000).
10. M. Afsal, C. Wang, L. Chu, H. Ouyang, and L. Chen, *J. Mater. Chem.* 22, 8420 (2012).
11. A. Singh, *Solid State Electron.* 28, 223 (1985).
12. M.M. Bülbül, S. Zeyrek, Ş. Altındal, and H. Yüzer, *Microelectron. Eng.* 83, 577 (2006).
13. P. Cova and A. Singh, *J. Appl. Phys.* 82, 5217 (1997).
14. D. Sands, K.M. Brunson, and M.H. Najaran, *Semicond. Sci. Technol.* 7, 1091 (1992).
15. J. Osvald and E. Burıan, *Solid- State Electronics* 42, 191 (1998).
16. S. Bengi and M.M. Bülbül, *Cur Appl. Phys.* 13, 1819 (2013).
17. E.H. Nicollian, *Mos (Metal Oxide Semiconductor) Physics and Technology* (New York: Wiley- Interscience, 2002).
18. M. Depas, R.L. Van Meirhaeghe, W.H. Laflere, and F. Cardon, *Semicond. Sci. Technol.* 7, 1476 (1992).
19. S. Ashok, J.M. Borrego, and R.J. Gutmann, *Solid State Electron.* 22, 621 (1979).
20. W. Divigalpitiya, *Sol. Energy Mater.* 18, 253 (1989).
21. H.M. Xiong, Y. Xu, O.G. Ren, and Y.Y. Xia, *J. Am. Chem. Soc.* 130, 7522 (2008).
22. Z.K. Tang, G.K.L. Wong, P. Yu, M. Kawasaki, A. Ohtomo, H. Koinuma, and Y. Segawa, *Appl. Phys. Lett.* 72, 3270 (1998).
23. Z.L. Wang, X.Y. Kong, Y. Ding, P.X. Gao, W.L. Hughes, R.S. Yang, and Y. Zhang, *Adv. Function. Mater.* 14, 943 (2004).
24. J.C. Johnson, H.Q. Yan, P.D. Yang, and R.J. Saykally, *J. Phys. Chem. B* 107, 8816 (2003).
25. X.D. Wang, C.J. Summers, and Z.L. Wang, *Nano Lett.* 4, 423 (2004).
26. S. Bilge Ocak, A.B. Selçuk, G. Aras, and E. Orhan, *Mater. Sci. Semicond. Process.* 38, 249 (2015).
27. E.H. Nicollian and J.R. Brews, *Solid-State Electron.* 27, 953 (1984).
28. S.A. Yeriskin, H. Ibrahim Unal, and B. Sari, *J. Appl. Poly. Sci.* 120, 390 (2011).
29. I.M. Afandiyeva, I. Dökme, Ş. Altındal, M.M. Bülbül, and A. Tataroğlu, *Microelectron. Eng.* 85, 247 (2008).
30. A. Kaya, S. Alialy, S. Demirezen, M. Balbaşı, S.A. Yerişkin, and A. Aytimur, *Ceram. Inter.* 42, 3322 (2016).
31. E. Arslan, S. Bütün, Y. Safak, and E. Özbay, *J. Electron. Mater.* 39, 2681 (2010).
32. P.S. Ho, E.S. Yang, H.L. Evans, and X. Wu, *Phys. Rev. Lett.* 60, 177 (1986).
33. J. Werner, A.F.J. Levi, R.T. Tung, M. Anzlowar, and M. Pinto, *Phys. Rev. Lett.* 60, 53 (1988).
34. P. Chattopadhyay and B. Raychaudhuri, *Solid State Electron.* 1992, 35 (1992).
35. W.A. Hill and C.C. Coleman, *Solid State Electron.* 23, 915 (1980).
36. M. Sharma and S.K. Tripathi, *Mater. Sci. Semicond. Process.* 41, 155 (2016).

37. N. Shiwakoti, A. Bobby, K. Asokan, and B. Antony, *Mater. Sci. Semicond. Process.* 42, 378 (2016).
38. H.G. Çetinkaya, S. Alialy, Ş. Altındal, A. Kaya, and İ. Uslu, *J. Mater. Sci.: Mater. Electron.* 26, 3186 (2015).
39. M. Asghar, K. Mahmood, F. Malik, and M.A. Hasan, 6th vacuum and surface sciences conference of Asia and Australia (VASSCAA-6). *J. Phys. Conf. Ser.* 439, 012031 (2013).
40. R. Singh, P. Sharma, Md A. Khan, V. Garg, V. Awasthi, A. Kranti, S. Mukherjee, *J. Phys. D: Appl. Phys.* 49, 445305 (2016).
41. L. Rajan, *IEEE Trans. Nanotechnol*. 15, 201 (2016).